## Title

CURVE CROSSING OF THE B 3u- ~ AND 3* STATES OF 0o AND ITS RELATION TO PREDISSOCIATION IN THE SCHUMANN-RUNGE BANDS



## Authors

Schaefer, Henry F.
Miller, William H.

## Publication Date

1971-06-01

Submitted to Journal of
Chemical Physics

UCRL-20598
Preprint



# CURVE CROSSING OF THE B $^3\Sigma_u^-$ AND $^3\Pi_u$ STATES OF $O_2$ AND ITS RELATION TO PREDISSOCIATION IN THE SCHUMANN-RUNGE BANDS

Henry F. Schaefer III and William H. Miller

June 1971

AEC Contract No. W-7405-eng-48



LAWRENCE RADIATION LABORATORY
UNIVERSITY of CALIFORNIA BERKELEY

## DISCLAIMER

# Curve Crossing of the B $^3\Sigma_u^-$ and $^3\Pi_u$ States of $O_2$ and Its Relation to Predissociation in the Schumann-Runge Bands*

Henry F. Schaefer III

Department of Chemistry, University of California,
Berkeley, California 94720

and

William H. Miller**

Inorganic Materials Research Division of
the Lawrence Radiation Laboratory
and the Department of Chemistry,
University of California,
Berkeley, California 94720

*Supported by the University of California Committee on Research, the Petroleum Research Fund, the Research Corporation, and the Atomic Energy Commission.

**Alfred P. Sloan Fellow.

## Abstract

Nonempirical quantum mechanical calculations including electron correlation have been carried out for the lowest $^3\Sigma_u^-$ and $^3\Pi_u$ states of $O_2$. A relatively large basis set is used and 257 $^3\Sigma_u^-$ and 345 $^3\Pi_u$ symmetry-adapted configurations are included in the first-order wave functions. For the B $^3\Sigma_u^-$ state the theoretical spectroscopic constants (with experimental values in parentheses) are $T_e$ 6.16 eV (6.17), $D_e$ 0.76 eV (1.01), $r_e$ 1.64Å (1.60), $\omega_e$ 679 $cm^{-1}$ (709), and $B_e$ 0.783 $cm^{-1}$ (0.819). Neither state is well described by a single electron configuration and the B $^3\Sigma_u^-$ state is seen to have a normal (non-Rydberg) electron distribution. The calculated potential curves indicate that the repulsive $^3\Pi_u$ curve crosses the inner limb of the B $^3\Sigma_u^-$ curve. Analogous calculations on the repulsive $^1\Pi_u$ state yield a crossing of the outer limb of the B $^3\Sigma_u^-$. Since previous interpretations of the predissociation of B $^3\Sigma_u^-$ have suggested that $^3\Pi_u$ crosses the outer limb, this predissociation is discussed in some detail. It is concluded that spin-orbit coupling is the principal interaction responsible for the predissociation, so that all four repulsive states that dissociate to ground state atoms are expected to predissociate B $^3\Sigma_u^-$ to roughly the same degree.

## I. Introduction

Thirty-five years ago Flory[1] suggested that predissociation occurs in the Schumann-Runge ($B\ ^3\Sigma_u^- - X\ ^3\Sigma_g^-$) bands[2] of the oxygen molecule. Flory's argument[1] was based primarily on a) in the emission spectrum no bands having $v > 2$ for the $B\ ^3\Sigma_u^-$ state had been observed and b) absorption of light by $O_2$ leads to photochemical decomposition at a faster rate than can be accounted for by assuming collisions of photoactivated molecules. Furthermore, Flory suggested that the repulsive $^3\Pi_u$ state of $O_2$ was responsible for the predissociation and presented a potential energy diagram indicating that the $^3\Pi_u$ curve crosses the $B\ ^3\Sigma_u^-$ state on its outer limb. Flory's analysis has been the subject of controversy since its publication.[1]

At the time (1950) of publication of Herzberg's book on diatomic spectra, Flory's theory of predissociation in $B\ ^3\Sigma_u^-$ $O_2$ was not generally accepted.[3] At about that time Feast[4] reported the observation of emission bands $v' = 3$ and concluded that Flory's analysis was unsatisfactory. However, photochemical investigations of the effects of foreign gases on the formation of ozone from $O_2$ were interpreted by Volman[5] to support Flory's conclusions.

The first part of Flory's analysis was definitively confirmed by Wilkinson and Mulliken[6], who reported what they considered to be a strong predissociation in the $v' = 12$ level. They also inferred that predissociation takes place in the whole range of levels from $v' = 4$ to $v' = 11$. Wilkinson and Mulliken[6] suggested that the origin of the observed predissociation was

a crossing of the inner limb of the B state (at v'=12) by the repulsive $^3\Pi_u$ state. They further pointed out[6] that weaker predissociations of the B state by the $^5\Sigma_u^-$, $^1\Pi_u$, or $^5\Pi_u$ states might also be observable.

Another important paper on this subject appeared in 1959 by Carroll.[7] Carroll found an even stronger (that Wilkinson and Mulliken at v'=12) predissociation at v' = 4. He attributed this predissociation to a crossing of the outer limb of the B $^3\Sigma_u^-$ state between v'= 3 and v'= 4 by the $^3\Pi_u$ state. Thus Carroll concluded that Flory's analysis was correct in detail. Carroll also pointed out[7] the observed predissociations at both v' = 4 and v' = 12 might be explained by a single repulsive potential via a quantum mechanical treatment of the Franck-Condon principle.[8] In addition Carroll raised the possibility that the weaker v' = 12 predissociation might be caused by the $^5\Sigma_u^-$, $^1\Pi_u$, or $^5\Pi_u$ states.

More recent spectroscopic investigations[9-13] have confirmed the predissociations observed by Wilkinson and Mulliken[6] and by Carroll.[7] It is particularly noteworthy that Hudson and Carter[10] found all the levels of B $^3\Sigma_u^-$ $O_2$ from v = 3 to v = 17 were subject to predissociation, the individual rotational lines having half-widths varying from 0.5 to 2.3 $cm^{-1}$.

The only <u>ab initio</u> quantum mechanical calculations on the potential energy curves relevant to this problem are those of Schaefer and Harris.[14] They used a minimum basis set of Slater functions and performed essentially full configuration interaction (CI) calculations on the states of interest. These calculations[14] predict the $^3\Pi_u$ repulsive curve to cross the inner limb of the

B $^3\Sigma_u^-$ curve. The three other curves mentioned by Wilkinson and Mulliken[6], $^5\Sigma_u^-$, $^1\Pi_u$, and $^5\Pi_u$ were all predicted[14] to be repulsive and cross the outer limb of the B $^3\Sigma_u^-$ curve.

In independent investigations, Murrell and Taylor[15] and Riess and Ben-Aryeh[16] have recently applied the Franck-Condon principle to predissociation in the Schumann-Runge bands of $O_2$. Both authors have carried out numerical calculations[15,16] which demonstrate, in accordance with the early theoretical discussion of Rice[8], that intersection of the B $^3\Sigma_u^-$ state by a single repulsive curve may give rise to several maxima of predissociation probability (occuring at different vibrational levels of the B state). Assuming a single repulsive curve, the best agreement with the observed strong and weak predissociations at v' = 4 and v' = 11 is obtained from a curve crossing the outer limb of the B state near v' = 4.[15,16] Both sets of authors conclude (Murrell and Taylor[15] more emphatically) that the observed predissociations are due to the $^3\Pi_u$ state crossing the outer limb of the B $^3\Sigma_u^-$ potential curve. In related work, Child[17] has theoretically discussed predissociation from a semiclassical point of view and used the predicted repulsive $^3\Pi_u$ curve of Murrell and Taylor[15] to compute predissociation probabilities.

The most accurate and complete spectroscopic investigation of $O_2$ predissociation is the recent work of Ackerman and Biaume[13], who photographed the first fourteen Schumann-Runge bands, from 0-0 to 13-0. Their pattern of observed B state vibrational linewidths may imply predissociation for <u>all</u> the B state vibrational levels, but otherwise appears to be in good qualitative agreement with the predictions of Murrell and Taylor.[15] However, Ackerman

and Biame point out that their observed maxima at v' = 7 and v' = 11 may arise from superposition rather than predissociation. They conclude[13] that the experimental data "do not fully support" the theoretical results of Murrell and Taylor[15] and that some other type of experimental measurement is required to confirm the Murrell-Taylor analysis.

Related to the Schumann-Runge predissociation problem is the fact that[18] the $^3\Pi_u$ to X $^3\Sigma_g^-$ transition may be responsible for the major part of the $O_2$ continuum in the wavelength region 2000-1750Å. Ogawa[18] has recently investigated this continuum experimentally and discussed the shape of the $^3\Pi_u$ potential curve from this point of view. Although no definite conclusions are made[18], Ogawa states out that no appreciable part of the Schumann-Runge continuum is due to the X $^3\Sigma_g^-$ - $^3\Pi_u$ transition if the $^3\Pi_u$ curve crosses the outer limb of the B state curve between v = 3 and 4. The Franck-Condon factor of such a $^3\Pi_u$ - X $^3\Sigma_g^-$ transition would be rather small under such circumstances.

The purpose of the present research was to calculate <u>ab initio</u> potential curves for the B $^3\Sigma_u^-$ and $^3\Pi_u$ state of a much higher reliability than those of Schaefer and Harris.[14] This is now possible due to recent advances of a computational[19] and theoretical[20] nature with regard to the treatment of electron correlation in diatomic molecules. The primary conclusion of these calculations, details of which are presented in Section II, is that the $^3\Pi_u$ state almost certainly crosses the <u>inner</u> branch of the B $^3\Sigma_u^-$ state, in qualitative agreement with the earlier less accurate

calculations.[14] Since this finding seems to contradict some interpretations of the predissociation of the B state, Section III discusses this predissociation in some detail. The essential point here is that since spin-orbit coupling appears to be the dominant interaction responsible for the predissociation, coupling of the B $^3\Sigma_u^-$ state to all the repulsive states [$^1\Pi_u$, $^3\Pi_u$, $^5\Pi_u$, $^5\Sigma_u^-$] which dissociate to ground state atoms is expected to be of comparable strength. Any, and perhaps all, of these four states, therefore, may predissociate the B $^3\Sigma_u^-$ state.

## II. Ab Initio Calculation of Potential Curves

### A. Basis Set

The basis set is the same as that used in earlier calculations[20a] on the X $^3\Sigma_u^-$ ground state of $O_2$. It consists of four s, two p, and one d function on each oxygen atom. With this basis the Hartree-Fock energy of the $^3P$ state of O is reproduced to within 0.0001 hartree, but the calculated SCF energy for ground state $O_2$ at 2.3 bohrs internuclear separation lies 0.53 eV above the near Hartree-Fock energy of Cade.[21] This molecular basis set error of 0.53 eV appears to be responsible for the fact that our computed dissociation energy for $O_2$ was 4.72 eV, as opposed to the experimental value 5.21 eV. With this basis the CI energies for the $^3P$ and $^1D$ states of O are -74.81041 and -74.72936 hartrees.

### B. Selection of Configuration

As in earlier work[20], here we use first-order wave functions[22] to describe electron correlation in molecules. In principle such first-order wave functions include all configuration in which no more than one electron occupies an orbital beyond the

valence shell (n=2 for the oxygen atom). The virtue of this method for the selection of configurations is that it is essentially automatic (no guess work required) and increases only linearly with the number of basis functions.

For the B $^3\Sigma_u^-$ state the configurations included are seen in Table I. Most of the first 201 configurations can be described and single or double excitations from the configuration $1\sigma_g^2 1\sigma_u^2 2\sigma_g^2 2\sigma_u^2 3\sigma_g^2 1\pi_u^3 1\pi_g^3$. The first actual calculation showed a second configuration, $1\sigma_g^2 1\sigma_u^2 2\sigma_g^2 2\sigma_u^2 3\sigma_g 3\sigma_u 1\pi_u^4 1\pi_g^2$, to be very important. Therefore the last 56 configurations in Table I are single and double excitations from this second reference state.

Our basis set can usefully be divided into four types of orbitals

(1) core orbitals - $1\sigma_g$, $1\sigma_u$.

(2) semi-valence-orbitals - $2\sigma_g$, $2\sigma_u$.

(3) valence orbitals - $3\sigma_g$, $3\sigma_u$, $1\pi_u$, $1\pi_g$.

(4) higher orbitals - $4\sigma_g - 7\sigma_g$, $4\sigma_u - 7\sigma_u$, $2\pi_u$, $3\pi_u$, $2\pi_g$, $3\pi_g$.

All configurations involving $1\sigma_g^2 1\sigma_u^2$ plus only semi-valence or valence orbitals are included. As Table I shows only single excitations from the core orbitals are included in our first-order wave function.

Finally, from the occupied valence orbitals ($3\sigma_g^2 1\pi_u^3 1\pi_g^3$), double excitations to one unfilled valence ($3\sigma_u$, $1\pi_u$, or $1\pi_g$) and one higher orbital are included.

For the $^3\Pi_u$ state the same procedure was followed with respect to the $1\sigma_g^2 1\sigma_u^2 2\sigma_g^2 2\sigma_u^2 3\sigma_g^2 3\sigma_u 1\pi_u^4 1\pi_g$ reference state, yielding 254 configurations. The first $^3\Pi_u$ CI showed the $1\sigma_g^2 1\sigma_u^2 2\sigma_g^2 2\sigma_u^2 3\sigma_g^2 3\sigma_u 1\pi_u^2 1\pi_g^3$ configuration to be very important. Therefore the appropriate single and double excitations from the valence orbitals of this second reference state were added. For practical reasons, excitations to orbitals higher than $4\sigma_g$, $4\sigma_u$, $2\pi_u$, and $2\pi_g$ were not included. Natural orbital[23] analyses show that occupation numbers fall off rapidly after $4\sigma_u$. Thus 345 configurations were included in the $^3\Pi_u$ calculations.

C. Method of Calculation.

The one- and two-electron integrals were evaluated to an accuracy of $10^{-7}$ hartree using a completely numerical scheme.[19a] Construction of symmetry-adapted linear combinations of determinants was carried out by direct diagonalization of the operators $S^2 + (\frac{1}{2})\sigma_v$ for $^3\Sigma_u^-$ and $S^2$ for $^3\Pi_u$.[19b]

A special problem arose in these calculations in the computation of the lowest eigenvalue and eigenvector of the Hamiltonian matrix. The Nesbet-Shavitt algorithm[24,25] works exceedingly well for cases in which one configuration has a coefficience of 0.9 or greater. But when the wave function contains no dominant single configuration, one finds slow convergence or no convergence. However, Shavitt[26] has recently found that by varying each component of the eigenvector during each iteration[24,25], convergence can be obtained where the original algorithm fails. For larger internuclear separations, for both the $^3\Sigma_u^-$ and $^3\Pi_u$ states the original algorithm[24,25] failed but the modified version[26] yielded convergence in between 10 and 50 iterations.

The difficult problem of obtaining an optimum set of molecular orbitals (yielding a rapidly convergent CI expansion) was approximately solved using the iterative natural orbital procedure of Bender and Davidson.[27] For homonuclear diatomics it appears that excellent results can be obtained by starting with symmetry orbitals (even and odd combinations of Hartree-Fock atomic orbitals). In all cases the energy stabilized to within $10^{-4}$ hartree after no more than five natural orbital iterations.

D. Spectroscopic Constants for B $^3\Sigma_u^-$ $O_2$

The calculated total energies, seen in Table II, were used to predict spectroscopic constants for the B state. These are compared with experiment and the earlier calculations[14] and experiment[28] in Table III. Our calculated excitation energy $T_e$ is in very close agreement with experiment. The percentages of experiment for the other spectroscopic constants are 102.3% ($r_e$), 95.8% ($\omega_e$), 125.5% ($\omega_e x_e$), 95.6% ($B_e$), and 120.7% ($\alpha_e$). As expected, the correction terms $\omega_e x_e$ and $\alpha_e$ are somewhat less accurate than $r_e$, $\omega_e$, and $B_e$. We note that the experimental values of Albritton, Schmeltekopf, and Zare[28] were obtained by fitting the observed vibrational levels to an expression including the additional constants $\omega_e y_e$ and $\gamma_e$.

Our calculated dissociation energy is in much better agreement with experiment than the earlier ab initio work.[14] The difference between calculated and experimental $D_e$ is 0.245 eV, small enough to make it impossible to determine whether our error is due to our basis set or the indequacy of the first-order wave function concept.

## E. Electronic Structure Considerations

The B $^3\Sigma_u^-$ and $^3\Pi_u$ states lie higher (relative to the ground state) than the states of many-electron diatomic molecules for which ab initio potential curves of comparable accuracy have been previously reported.[20,29-31] Therefore it is of interest to see if the electronic structures of these two states display any unusual features. To this end, Table IV indicates the most important configurations in the two wave functions and Table V the natural orbital occupation numbers.

For the $^3\Pi_u$ state the most important configuration, as expected is the $3\sigma_g^2 3\sigma_u 1\pi_u^4 1\pi_g$. However, the second configuration $3\sigma_g^2 3\sigma_u 1\pi_u^2 1\pi_g^3$ is also very important near $r_e$ (3.1 bohrs). As is well known, Table IV shows that the single configuration approximation becomes very poor as the molecule dissociates. The occupation numbers at r = 3.1 indicate that the simplest accurate orbital picture of the $^3\Pi_u$ state is one in which $\sim 3\frac{1}{2}$ electrons occupy the $1\pi_u$ orbital and $\sim 1\frac{1}{2}$ electrons occpy the $1\pi_g$.

On the basis of CI calculations in the π-electron approximation, Taketa, et.al.[32] concluded that the B state of $O_2$ is a Rydberg or diffuse state. However, Morokuma and Konishi[33] have recently demonstrated that the B state is essentially a valence state. They showed[33] that forcing the $3\sigma_g$ orbital to be doubly occupied in all configurations (which amounts to the π-electron approximation in this case) puts an unrealistic constraint on the form of the wave function.

Table IV indicates that the electronic structure of the B $^3\Sigma_u^-$ state near $r_e$ is determined primarily by two configurations, $3\sigma_g^2 1\pi_u^3 1\pi_g^3$ and $3\sigma_g 3\sigma_u 1\pi_u^4 1\pi_g^2$. A third configuration,

$3\sigma_g 3\sigma_u 1\pi_u^2 1\pi_g^4$, is also quite important near $r_e$. Both the second and third B state configurations would not be included in a π-electron treatment. In addition, inspection of the actual wave function at r = 3.1 bohrs shows that the more diffuse basis functions appear no more important than in the ground state of $O_2$.[20] Thus the present work fully supports the conclusions of Morokuma and Konishi.[33]

It is pertinent to note here that the V state ($\pi\pi^*$ singlet) of ethylene is thought to be[32] in some ways analogous to the B state of $O_2$. While SCF calculations on the V state of $C_2H_4$ imply that it is Rydberg-like[34], it has been suggested[35] that the inclusion of electron correlation will result in a nearly normal valence-like state.

The B state natural orbital occupation numbers essentially describe the electronic structure near $r_e$ as $3\sigma_g^{1.69}\ 3\sigma_u^{0.35}\ 1\pi_u^{3.18}\ 1\pi_g^{2.78}$. Our results for B $^3\Sigma_u^-$ and $^3\Pi_u$ states of $O_2$ probably indicate a general trend--that the higher electronic states of molecules may (even near the equilibrium geometry) be very poorly described by a single electron configuration.

F. Potential Energy Curves

The predicted potential energy curves are shown in Figure 1. In addition to the $^3\Pi_u$ and $^3\Sigma_u^-$ curves, a $^1\Pi_u$ curve calculated by the same method[36] is shown in Figure 1. Also included in Figure 1 is the numerically tabulated experimental B $^3\Sigma_u^-$ curve obtained by Albritton, Schmeltekopf, and Zare.[28] In Figure 1, the calculated B $^3\Sigma_u^-$ curve has been uniformly lowered by 0.00875 hartrees or 0.238 eV. This is because our atomic calculations

(which yield the dissociation limits) predict the $^1D$ state to lie 2.205 eV above the $^3P$ state, whereas this splitting is experimentally known to be 1.967 eV.[37] Perhaps the best argument for the reliability of our calculations is that the ab initio and experimental[28] B state curves are nearly parallel.

Comparing the theoretical repulsive curves with either the theoretical or experimental B state curve yields the same qualitative result: the $^3\Pi_u$ curve crosses the inner limb while the $^1\Pi_u$ state crosses the outer limb of the B $^3\Sigma_u^-$ potential curve. It certainly appears that the present calculations are sufficiently accurate that these qualitative conclusions are correct. The exact positions of the two crossing points are much more difficult to assess. The crossing points can be most reasonably estimated by realizing that, relative to the experimental B state curve[28], the calculated $^3\Pi_u$ and $^1\Pi_u$ curves are likely to be somewhat too repulsive. Taking this into account one might conclude that the $^3\Pi_u$ curve crosses the inner limb of the B $^3\Sigma_u^-$ state curve somewhat above v = 4, while the $^1\Pi_u$ curve crosses the outer limb between v = 0 and v = 1. However, these estimates of the crossing points should be regarded as speculative and not essential to the primary conclusions of this research.

## III. Predissociation of the B $^3\Sigma_u^-$ State

Predissociation is one of the simplest examples of a "golden-rule", or radiationless transition--i.e., the decay of a metastable discrete state into a continuum state which is energetically degenerate with it.[38] The "width" associated with the discrete vibrational state (in units of energy) is

$$\Gamma = 2\pi |\langle n|V_{12}|k\rangle|^2 \rho, \tag{1}$$

where 1 and 2 denote the initial and final electronic states, n and k the initial (discrete) and final (continuous) vibrational states, and $V_{12}$ is the coupling between the two electronic states. The matrix element in Eq. (1) is given explicitly as an integral over internuclear distance

$$\langle n|V_{12}|k\rangle = \int_0^\infty dr\, f_n(r) V_{12}(r) g_k(r), \tag{2}$$

where $f_n(r)$ is normalized to unity, and if $g_k(r)$ is normalized such that at large r

$$g_k(r) \sim \sin(kr + \text{constant}), \tag{3}$$

then the density of final states in Eq. (1) is

$$\rho = 2\mu/(\hbar^2 k\pi), \tag{4}$$

where $k = (2\mu E_2/\hbar^2)^{\frac{1}{2}}$, $E_2$ being the final asymptotic translational energy of the nuclei and $\mu$ being their reduced mass.

The physical meaning of $\Gamma$ is that $(\hbar/\Gamma)$ is the average time the discrete state exists before it predissociates. More precisely, if the state is observed spectroscopically, then spectral lines involving transitions to or from it will be Lorentzian with a full-width at half-height given by $\Gamma$ (i.e., $\Delta\nu = \Gamma/h$) provided, of course, that line broadening from all other sources is much smaller than that from predissociation.

If the potential curves $V_1(r)$ and $V_2(r)$ [i.e., the electronic eigenvalues as a function of internuclear distance] cross[39] at internuclear distance $r_x$, then it is well-known[40] that the region of r about $r_x$ gives the dominant contribution to the integral in Eq. (2), so that

$$\Gamma = 2\pi \, |V_{12}(r_x)|^2 |\langle n|k\rangle|^2 \rho; \qquad (5)$$

i.e., the electronic and nuclear contributions to the width enter multiplicatively in this approximation. First we discuss the electronic factor, and then the nuclear, or Franck-Condon factor.

A. Electronic Selection Rules

Landau and Lifshitz[40] have given by far the clearest discussion of the nature of the electronic coupling, $V_{12}$ of Eq. (5). There are essentially two interactions which can couple Born-Oppenheimer states of different symmetry and thus give rise to predissociation: (1) orbit-rotation coupling, the coriolis interaction of the electronic orbital angular momentum with the rotational angular momentum of the nuclei, and (2) spin-orbit coupling, the purely electronic interaction of the spin and orbital angular momentum of the electrons. For both these interactions one has the selection rules that total angular momentum and the sign of the state cannot change. For homonuclear diatomic molecules, one has in addition conservation of parity (i.e., $g \leftrightarrow u$ transitions are forbidden).

For the orbit-rotation interaction one in addition has the selection rules[40]

$$\Delta S = 0; \; \Delta\Lambda = \pm 1, \qquad (6)$$

where S is the total electronic spin and $\Lambda$ is the component of electronic orbital angular momentum along the internuclear axis. These are the often-quoted[41] Krönig selection rules for predissociation and are valid only if this interaction is the dominant one. The magnitude of the orbit-rotation coupling is given roughly by

$$V_{12}^{O-R}(r_x) \simeq (\hbar^2/2\mu r_x^2)\,2J|\Delta\Lambda| = J\hbar^2/\mu r_x^2, \qquad (7)$$

where J is the rotational quantum number.

The spin-orbit interaction, on the other hand, has selection rules[40]

$$\Delta S = 0, \pm 1; \ \Delta\Lambda = 0, \pm 1, \qquad (8)$$

with not both $\Delta S$ and $\Delta\Lambda = 0$ if $\Lambda \neq 0$; $\Sigma^+ \leftrightarrow \Sigma^-$ is allowed, however, for $\Delta S = 0$ as well as $\pm 1$. Since this interaction involves only electronic degrees of freedom, it is independent of J, and this feature is its "signature". There is no simple way to estimate the magnitude of the spin-orbit interaction in a molecule; there is no reason, however, to expect the coupling between all states connected by these selection rules to differ greatly in magnitude.

The total electronic interaction can therefore be written in the form

$$V_{12}(r_x) = aJ + b \qquad (9)$$

where a and b are non-zero only if electronic states 1 and 2 obey the selection rules in Eqs. (6) and (8), respectively. There are two principal handles one can use to decide which interaction is dominant and thus which selection rules are most relevant: (1) the J dependence of the interaction, and (2) the fact that one has a good estimate for the magnitude of the orbit-rotation coupling. If, for example, the predissociation width is larger than can be accounted for by the value of $a \simeq \hbar^2/\mu r_x^2$ and if the interaction appears to be independent of J, then one concludes that the spin-orbit interaction is dominant and the pertinent selections rules are those given by Eq. (8). This appears to be the case for predissociation of the $B\ ^3\Sigma_u^-$ state of $O_2$, at least for J not too large (see sub-section C below).

B. The Franck-Condon Factor

The second factor in Eq. (5), the square of the overlap integral of the two vibrational wavefunctions, is the familiar Franck-Condon (FC) factor. It appears in many phenomena involving electronic transitions and is a result of the sudden approximation--i.e., that the elctronic transition takes place essentially instantaneously with respect to motion of the nuclei. The FC factor is, of course, completely unrelated to the nature of the electronic coupling and the selection rules pertaining thereto.

Since the vibrational wavefunctions describe motion of nuclei, a semiclassical approximation is quite appropriate for evaluation of the FC factor.[40,42] A uniform semiclassical approximation has also been devised[43], and this gives

$$2\pi\rho|\langle n|k\rangle|^2 = (2\mu/\hbar^2 k_x)\varepsilon'(n)|V_1'-V_2'|^{-1}2\pi Z^{\frac{1}{2}}Ai^2(-Z), \quad (10)$$

where $\varepsilon(n)$ is the vibrational eigenvalue function for the discrete state, $k_i(r) = \{2\mu[E-V_i(r)]/\hbar^2\}^{\frac{1}{2}}$, $V_i' = V_i'(r_x)$, $k_x$ is the common value of $k_1(r)$ and $k_2(r)$ at the crossing point, and

$$Z = (\tfrac{3}{2}\tau)^{\frac{2}{3}}; \quad (11)$$

$\tau$ is a phase integral related to the two intersecting potential curves.

If the two potentials intersect as in Fig. 2a, then

$$\tau = \int_{r_2}^{r_x} dr\ k_2(r) + \int_{r_x}^{r_{1>}} dr\ k_1(r), \quad (12)$$

and if the intersection is as in Fig. 2b, then

$$\tau = \int_{r_{1<}}^{r_x} dr\ k_1(r) - \int_{r_2}^{r_x} dr\ k_2(r). \quad (13)$$

The "potential wells" associated with these phase integrals are indicated by the shaded regions in Fig. 2.

If one approximates the two potentials as <u>linear</u> functions about the crossing point, then Eq. (10 becomes

$$2\pi\rho|\langle n|k\rangle|^2 = 2\pi(2\mu/\hbar^2)^{\frac{2}{3}}\varepsilon'(n)|V_1'-V_2'|^{-\frac{2}{3}}|V_1'V_2'|^{-\frac{1}{3}} \times Ai^2(-Z), \tag{14}$$

where

$$Z = (2\mu/\hbar^2)^{\frac{1}{3}}\left|\frac{1}{V_2'} - \frac{1}{V_1'}\right|^{\frac{2}{3}}[E - V_x], \tag{15}$$

and $V_x = V_1(r_x) = V_2(r_x)$. [Eqs. (14) and (15) would be quite useful in understanding <u>isotope effects</u> in FC factors.] One should note that Eqs. (14) and (15) are also meaningful if $E < V_x$--i.e., if the energy is <u>below</u> that of the crossing point. In this case $Z < 0$, so that the Airy function is exponentially decreasing[44]; i.e., the nuclei must "tunnel" in order to predissociate.

Interest has centered recently on "secondary maxima" in the FC factor. From the general nature of the Airy function[44] it is clear how these arise, for Z is a monotonically increasing functional of vibrational quantum number n. Their physical origin, however, is more apparent if one examines the "primitive semi-classical" expression[40], obtained by employing the asymptotic approximation for the Airy function[44]; the only modification of Eq. (10) is the replacement

$$\pi Z^{\frac{1}{2}}Ai^2(-Z) \rightarrow \sin^2(\tfrac{\pi}{4} + \tau) = \tfrac{1}{2} + \tfrac{1}{2}\sin(2\tau)$$

$$= \text{classical result} + \text{interference}.$$

The phase of the interference term is the difference in the classical actions associated with the two different paths (or trajectories) by which predissociation can occur. To see this, consider Fig. 2a, for example, and suppose the particle starts

out at $r = r_{1<}$. Path I is from $r_{1<}$ to $r_x$ on $V_1$, crossing to $V_2$ at $r_x$, and from $r_x$ to $\infty$ on $V_2$. Path II is from $r_{1<}$ to $r_{1>}$ on $V_1$ (not crossing at $r_x$), $r_{1>}$ to $r_x$ on $V_1$, crossing to $V_2$ at $r_x$, $r_x$ to $r_2$ on $V_2$, and from $r_2$ to $\infty$ on $V_2$ (not crossing at $r_x$). The classical actions associated with these two paths are

$$\phi_I = \int_{r_{1<}}^{r_x} dr\ k_1(r) + \int_{r_x}^{\infty} dr\ k_2(r)$$

$$\phi_{II} = \int_{r_{1<}}^{r_{1>}} dr\ k_1(r) + \int_{r_x}^{r_{1>}} dr\ k_1(r) + \int_{r_2}^{r_x} dr\ k_2(r) + \int_{r_2}^{\infty} dr\ k_2(r),$$

and it is a simple matter to show that $\phi_{II} - \phi_I = 2\tau$, where $\tau$ is given by Eq. (13).

Child[17] has recently pointed out that determination of these interference features in the FC factor is essentially a measurement of the phase integral $\tau$ as a function of energy. As such, it is in principle possible to employ the RKR inversion formulae[45] to determine the repulsive potential $V_2(r)$ directly from experimental data (provided $V_1(r)$ is known). More recently, Miller[46] has given additional inversion formulae, analogous to the RKR expressions, which also use experimentally determined phase integrals to obtain potential curves.

In practice, however, the data is often so far short of perfect that these analytical inversion formulae are not necessarily useful. Murrell and Taylor[15] have recently applied a "brute-force" approach with some success: a functional form with adjustable parameters was assumed for $V_2(r)$ and FC factors computed for various choices of the parameters. For predissociation of the

B $^3\Sigma_u^-$ state of $O_2$ they succeeded in obtaining maxima in the FC factors for vibrational levels n = 4, 7, and 11. [They designated the repulsive curve as the $^3\Pi_u$ state, but the symmetry of the repulsive state is, of course, unrelated to structure in the FC factor; their repulsive curve is the dashed line in Fig. 1.] These maxima agree quite well with the predissociation widths measured by Ackerman and Biaume[13], although these quthors note that these secondary maxima may arise from effects other than via interference structure in the FC factor.

### C. Discussion for the B $^3\Sigma_u^-$ State of $O_2$

The main point to be established is that spin-orbit coupling is the dominant interaction causing the predissociation. First, the predissociation widths appear to be independent of J.[15] Second, a rough estimate of the magnitude of the electronic coupling can be made by using the line width measurements of Ackerman and Biaume.[13] The maximum line width near the n = 4 vibrational level is $\Gamma$ = 8 $cm^{-1}$ (their value of 4 $cm^{-1}$ is the half-width at half-height). Since this corresponds to an energy just above the crossing point, one can use the "linearized approximation" to the FC factor, Eqs. (14) and (15). This maximum width corresponds to the Airy function in Eq. (14) taking on its first maximum, Ai = .53566. Combining Eq. (5) with Eq. (14), one thus has

$$\Gamma = V_{12}(r_x)^2 2\pi(2\mu/\hbar^2)^{\frac{2}{3}}\, \varepsilon'(n)\,|V_1'-V_2'|^{-\frac{2}{3}}|V_1'V_2'|^{-\frac{1}{3}}Ai^2, \quad (16)$$

where

$$\Gamma \simeq 8\ cm^{-1} \simeq 3.65 \times 10^{-5}\ \text{hartree}$$

$$Ai = .53566$$

$$\mu \simeq 8\ \text{amu};$$

using Murrell and Taylor's[15] potential for $V_2(r)$ [the dashed curve in Fig. 1] and the known B $^3\Sigma_u^-$ potential, one has the approximate values

$$\varepsilon'(n) \simeq 0.0027 \text{ hartree}$$

$$V_1'(r_x) \simeq 0.030 \text{ hartree/bohr}$$

$$V_2'(r_x) \simeq -0.084 \text{ hartree/bohr.}$$

With these values substituted into Eq. (16) one finds the electronics coupling to be

$$V_{12}(r_x) \simeq 110 \text{ cm}^{-1}.$$

[Even if only half of the line width is assumed to result from this particular curve crossing near n = 4, the inferred value of $V_{12}$ is reduced only to 78 $\text{cm}^{-1}$.] The orbit-rotation interaction has a magnitude $J\hbar^2/\mu r_x^2$, and with $r_x \simeq 3.6\ a_o$, this is about $1.2J\ \text{cm}^{-1}$. At room temperature the most probable value of J for ground state $O_2$ is $\sim$8, so that the orbit-rotation interaction is on the order of 10 $\text{cm}^{-1}$, and presumably too small to explain the observed predissociation widths. On the basis of its magnitude and its J dependence, therefore, the electronic interaction responsible for the predissociation appears to be spin-orbit coupling.

This conclusion is also consistent with our calculated $^3\Pi_u$ state, which does <u>not</u> cross the outer branch of the B $^3\Sigma_u^-$ state; $^3\Pi_u$ is the only state that would be coupled to $^3\Sigma_u^-$ by the orbit-rotation selection rules [Eq. (6)], but the spin-orbit selection rules [Eq. (8)] also couple the other three repulsive states [$^1\Pi_u$, $^5\Pi_u$, and $^5\Sigma_u^-$] which dissociate to ground state atoms.

These three states do cross the outer branch of the B $^3\Sigma_u^-$ state.

In addition to the predissociation maxima seen by Ackerman and Biaume[13], at n = 4, 7, and 11, most workers agree that all vibrational levels n = 3 to 17 are predissociated to some extent. This could very well be a result of the $^3\Pi_u$ state which intersects the inner branch of B $^3\Sigma_u^-$, the two potentials being so nearly parallel that the first maximum of the Airy function in Eq. (10) is a broad maximum spread out over all the vibrational levels of B $^3\Sigma_u^-$; this is the interpretation advanced by Wilkinson and Mulliken.[6] The predissociation maxima at levels n = 4, 7, and 11 are superimposed on this broad background. If these maxima are the result of interference in the FC factor associated with a crossing of the outer branch just below n = 4 [the dashed curve in Fig. 1], the question remains as to which repulsive state this is. Our calculations indicate rather conclusively that $^3\Pi_u$ crosses on the inner branch and (less conclusively) that $^1\Pi_u$ crosses too low on the outer branch to be the state in question. The two quintet states, $^5\Pi_u$ and $^5\Sigma_u^-$, both lie above[14] $^1\Pi_u$, and one of these could conceivably cross near n = 4. As Ackerman and Biaume[13] have cautioned, however, it is also possible that these maxima arise solely from experimental difficulties and are unrelated to any interference effects in the FC factor associated with a single crossing. It is clear that more detailed experimental information is necessary to resolve all these questions.

## Acknowledgements

We thank Professor Richard N. Zare for a copy of relevant sections of his book[28] prior to publication and Professor I. Shavitt for an illuminating discussion on the calculation of eigenvalues and eigenvectors. H.F.S. thanks the Nuclear Chemistry Division, Lawrence Radiation Laboratory, Berkeley for a generous grant of computer time.

## References


1. P.J. Flory, J. Chem. Phys. 4, 23 (1936).
2. V. Schumann, Smithsonian Contrib. Knowl. 29, No. 1413 (1903); C. Runge, Physica 1, 254 (1921).
3. G. Herzberg, Spectra of Diatomic Molecules (D. Van Nostrand Co., New York, 1950).
4. M.W. Feast, Proc. Roy. Soc. (London) A62, 114 (1949); A63, 549 (1950).
5. D.H. Volman, J. Chem. Phys. 24, 122 (1956); 25, 288 (1956).
6. P.G. Wilkinson and R.S. Mulliken, Astrophys. J. 125, 594 (1957).
7. P.K. Carroll, Astrophys. J. 129, 794 (1959).
8. O.K. Rice, J. Chem. Phys. 1, 375 (1933).
9. G.W. Bethke, J. Chem. Phys. 31, 669 (1959).
10. R.D. Hudson, V.L. Carter, and J.A. Stein, J. Geophys. Res. 71, 2295 (1966); R.D. Hudson and V.L. Carter, J. Opt. Soc. Am. 58, 1621 (1968); Can. J. Chem. 47, 1840 (1969).
11. Y. Ben-Aryeh, J. Opt. Soc. Am. 58, 679 (1968).
12. V. Hasson, G.R. Hebert, and R.W. Nicholls, J. Phys. B 3, 1188 (1970).
13. M. Ackerman and F. Biaume, J. Mol. Spectry. 35, 73 (1970).
14. H.F. Schaefer and F.E. Harris, J. Chem. Phys. 48, 4946 (1968).
15. J.N. Murrell and J.M. Taylor, Mol. Phys. 16, 609 (1969).
16. I.Riess and Y. Ben-Aryeh, J. Quant. Spectry. Radiative Transfer 9, 1463 (1969).
17. M.S. Child, J. Mol. Spectry. 33, 487 (1970).
18. M. Ogawa, J. Chem. Phys. 54, 2550 (1971).
19. H.F. Schaefer, (a) J. Chem. Phys. 52, 6241 (1970); (b) J. Computational Phys. 6, 142 (1970).

20. H.F. Schaefer, (a) J. Chem. Phys. 54, 2207 (1971); (b) 55, oooo (1971).

21. P.E. Cade, unpublished.

22. H.F. Schaefer and F.E. Harris, Phys. Rev. Letters 21, 1561 (1968).

23. P.O. Löwdin, Phys. Rev. 97, 1474 (1955).

24. R.K. Nesbet, J. Chem. Phys. 43, 311 (1965).

25. I. Shavitt, J. Computational Phys. 6, 124 (1970).

26. I. Shavitt, unpublished.

27. C.F. Bender and E.R. Davidson, J. Phys. Chem. 70, 2675 (1966).

28. D.L. Albritton, A.L. Schmeltekopf, and R.N. Zare, Diatomic Intensity Factors, in preparation.

29. P.J. Bertoncini, G. Das, and A.C. Wahl, J. Chem. Phys. 52, 5112 (1970).

30. G. Das and A.C. Wahl, Phys. Rev.Letters 24, 440 (1970).

31. B. Liu and H.F. Schaefer, J. Chem. Phys. 55, oooo (1971).

32. H. Taketa, H. Takewaki, O. Nomura, and K. Ohno, Theoretica Chimica Acta 11, 369 (1968).

33. K. Morokuma and H. Konishi, J. Chem. Phys. 55, oooo (1971).

34. T.H. Dunning, W.J. Hunt, and W.A. Goddard, Chem. Phys. Letters 4, 146 (1969).

35. H. Basch and V. McKoy, J. Chem. Phys. 53, 1628 (1970).

36. For the $^1\Pi_u$ calculations, the 97 orbital occupancies used were the same as those described above for $^3\Pi_u$. The number of resulting $^1\Pi_u$ symmetry eigenfunctions was 248. The 248 configuration energies were -149.56337 (r=3.1), -149.57736 (r=3.3), -149.58797 (r=3.5), and -149.60553 (r=4.0 bohrs).

37. C.E. Moore, "Atomic Energy Levels", Nat. Bur. Std. (U.S.) Circ. No. 467 (1949).

38. See, for example, L.I. Schiff, Quantum Mechanics (McGraw-Hill, New York, 1968) pp. 283-285.

39. If there is no value of r for which $V_1(r) = V_2(r)$, then the width is too small for predissociation to be a signif-cant effect.

40. L.D. Landau and E.M. Lifshitz, Quantum Mechanics (Addison-Wesley, Reading, Mass., 1965) pp. 322-330.

41. See, for example, reference 3, pp. 416-419.

42. See also M.S. Child, Mol. Phys. 8, 517 (1964).

43. W.H. Miller, J. Chem. Phys. 48, 464 (1968).

44. M. Abramowitz and I.A. Stegun, Handbook of Mathematical Functions (U.S. Government Printing Office, Washington, 1964) pp. 446-449.

45. See, for example, E.A. Mason and L. Monchick, Adv. Chem. Phys. 12, 351 (1967).

56. W.H. Miller, J. Chem. Phys. 54, oooo (1971).

Table I. Configurations included in the variational wave function for the $B\ ^3\Sigma_u^-$ state of $O_2$.

| Type excitation | $^3\Sigma_u^-$ configurations per orbital occupancy | Total Configurations |
|---|---|---|
| $1\sigma_g^2 1\sigma_u^2 2\sigma_g^2 2\sigma_u^2 3\sigma_g^2 1\pi_u^3 1\pi_g^3$ | 1 | 1 |
| core single excitations | | |
| $1\sigma_g, 2\sigma_g \rightarrow 4\sigma_g, 5\sigma_g, 6\sigma_g, 7\sigma_g$ | 1 | 8 |
| $1\sigma_u \rightarrow 3\sigma_u, 4\sigma_u, 5\sigma_u, 6\sigma_u, 7\sigma_u$ | 1 | 5 |
| $2\sigma_u \rightarrow 4\sigma_u, 5\sigma_u, 6\sigma_u, 7\sigma_u$ | 1 | 4 |
| semi-valence to valence single excitation | | |
| $2\sigma_u \rightarrow 3\sigma_u$ | 3 | 3 |
| valence to higher single excitations | | |
| $3\sigma_g \rightarrow 4\sigma_g, 5\sigma_g, 6\sigma_g, 7\sigma_g$ | 3 | 12 |
| $1\pi_u \rightarrow 2\pi_u, 3\pi_u$ | 4 | 8 |
| $1\pi_g \rightarrow 2\pi_g, 3\pi_g$ | 4 | 8 |

Table I Cont'd.

| | | |
|---|---|---|
| **double excitations from valence or semi-valence orbitals into valence orbitals** | | |
| $2\sigma_g^2, 2\sigma_u^2, 3\sigma_g^2 \rightarrow 3\sigma_u^2$ | 1 | 3 |
| $2\sigma_g 3\sigma_g \rightarrow 3\sigma_u^2$ | 3 | 3 |
| $1\pi_u^2, 1\pi_g^2 \rightarrow 3\sigma_u^2$ | 1 | 2 |
| $2\sigma_g 1\pi_u, 3\sigma_g 1\pi_u \rightarrow 3\sigma_u 1\pi_g$ | 2 | 4 |
| $2\sigma_g 1\pi_g, 3\sigma_g 1\pi_g \rightarrow 3\sigma_u 1\pi_u$ | 2 | 4 |
| **triple excitations from valence or semi-valence orbitals into valence orbitals** | | |
| $2\sigma_g 2\sigma_u 1\pi_g \rightarrow 3\sigma_u^2 1\pi_u$ | 2 | 2 |
| $2\sigma_u 3\sigma_g 1\pi_g \rightarrow 3\sigma_u^2 1\pi_u$ | 2 | 2 |
| $2\sigma_g 2\sigma_u 1\pi_u \rightarrow 3\sigma_u^2 1\pi_g$ | 2 | 2 |
| $2\sigma_u 3\sigma_g 1\pi_u \rightarrow 3\sigma_u^2 1\pi_g$ | 2 | 2 |
| **double excitations from two valence orbitals into one valence and one higher orbital** | | |
| $3\sigma_g^2 \rightarrow 3\sigma_u 4\sigma_u, 3\sigma_u 5\sigma_u, 3\sigma_u 6\sigma_u, 3\sigma_u 7\sigma_u$ | 3 | 12 |
| $3\sigma_g^2 \rightarrow 1\pi_u 2\pi_u, 1\pi_u 3\pi_u$ | 1 | 2 |
| $3\sigma_g^2 \rightarrow 1\pi_g 2\pi_g, 1\pi_g 3\pi_g$ | 1 | 2 |

Table I Cont .

| | | |
|---|---|---|
| $3\sigma_g 1\pi_u \rightarrow 3\sigma_u 2\pi_g, 3\sigma_u 3\pi_g$ | 12 | 24 |
| $3\sigma_g 1\pi_u \rightarrow 1\pi_g 4\sigma_u, 1\pi_g 5\sigma_u, 1\pi_g 6\sigma_u, 1\pi_g 7\sigma_u$ | 2 | 8 |
| $3\sigma_g 1\pi_g \rightarrow 3\sigma_u 2\pi_u, 3\sigma_u 3\pi_u$ | 12 | 24 |
| $3\sigma_g 1\pi_g \rightarrow 1\pi_u 4\sigma_u, 1\pi_u 5\sigma_u, 1\pi_u 6\sigma_u, 1\pi_u 7\sigma_u$ | 2 | 8 |
| $1\pi_u^2 \rightarrow 3\sigma_u 4\sigma_u, 3\sigma_u 5\sigma_u, 3\sigma_u 6\sigma_u, 3\sigma_u 7\sigma_u$ | 3 | 12 |
| $1\pi_u^2 \rightarrow 1\pi_g 2\pi_g, 1\pi_g 3\pi_g$ | 1 | 2 |
| $1\pi_u 1\pi_g \rightarrow 3\sigma_u 4\sigma_g, 3\sigma_u 5\sigma_g, 3\sigma_u 6\sigma_g, 3\sigma_u 7\sigma_g$ | 5 | 20 |
| $1\pi_g^2 \rightarrow 3\sigma_u 4\sigma_u, 3\sigma_u 5\sigma_u, 3\sigma_u 6\sigma_u, 3\sigma_u 7\sigma_u$ | 3 | 12 |
| $1\pi_g^2 \rightarrow 1\pi_u 2\pi_u, 1\pi_u 3\pi_u$ | 1 | 2 |
| CONFIGURATIONS ADDED BASED ON THE IMPORTANCE OF $1\sigma_g^2 1\sigma_u^2 2\sigma_g^2 2\sigma_u^2 3\sigma_g 3\sigma_u 1\pi_u^4 1\pi_g^2$ | | |
| valence to higher single excitations | | |
| $3\sigma_g \rightarrow 4\sigma_g, 5\sigma_g, 6\sigma_g, 7\sigma_g$ | 2 | 8 |
| $1\pi_g \rightarrow 2\pi_g, 3\pi_g$ | 3 | 6 |

Table I Cont'd.

double excitations from two valence orbitals into one valence and one higher orbital.

| | | |
|---|---|---|
| $3\sigma_g 1\pi_u \rightarrow 3\sigma_u 2\pi_g, 3\sigma_u 3\pi_g$ | 4 | 8 |
| $3\sigma_g 1\pi_g \rightarrow 3\sigma_u 2\pi_u, 3\sigma_u 3\pi_u$ | 1 | 2 |
| $1\pi_u^2 \rightarrow 3\sigma_u 4\sigma_u, 3\sigma_u 5\sigma_u, 3\sigma_u 6\sigma_u, 3\sigma_u 7\sigma_u$ | 5 | 20 |
| $1\pi_u 1\pi_g \rightarrow 3\sigma_u 4\sigma_g, 3\sigma_u 5\sigma_g, 3\sigma_u 6\sigma_g, 3\sigma_u 7\sigma_g$ | 3 | 12 |
| TOTAL | | 257 |

Table II. Total energies (in hartrees) for the lowest $^3\Pi_u$ and B $^3\Sigma_u^-$ states of $O_2$.

| | $^3\Pi_u$ | | B $^3\Sigma_u^-$ | |
|---|---|---|---|---|
| R (bohrs) | First Natural Configuration | 257 Configurations | First Natural Configuration | 345 Configurations |
| 2.5 | -149.30330 | -149.50960 | -149.20808 | -149.51780 |
| 2.6 | -149.32043 | -149.54006 | -149.20712 | -149.53680 |
| 2.7 | -149.32911 | -149.56233 | -149.20090 | -149.55001 |
| 2.9 | -149.32836 | -149.58925 | -149.17757 | -149.56417 |
| 3.1 | -149.31222 | -149.60132 | -149.14344 | -149.56776 |
| 3.3 | -149.28775 | -149.60584 | -149.10843 | -149.56560 |
| 3.5 | -149.25924 | -149.60755 | -149.07308 | -149.56089 |
| 4.0 | -149.18598 | -149.61253 | -149.98459 | -149.54938 |
| $\infty$ | | -149.62082 | | -149.53977 |

Table III. Theoretical and experimental spectroscopic constants for the $B\ ^3\Sigma_u^-$ state of $O_2$. The calculated total energies are those at 3.1 bohrs internuclear separation.

| | E(hartrees) | $T_e$(eV) | $D_e$(eV) | $r_e$(Å) | $\omega_e$($cm^{-1}$) | $\omega_e x_e$($cm^{-1}$) | $B_e$($cm^{-1}$) | $\alpha_e$($cm^{-1}$) |
|---|---|---|---|---|---|---|---|---|
| Full CI, minimum basis[a] | -148.9980 | 6.06 | 0.30 | 1.68 | 593 | -27 | 0.74 | 0.012 |
| First-order, this work | -149.5678 | 6.16 | 0.762 | 1.641 | 679 | 13.3 | 0.783 | 0.0146 |
| Experiment[b] | | 6.17 | 1.007 | 1.604 | 709 | 10.6 | 0.819 | 0.0121 |

[a] H.F. Schaefer and F.E. Harris, J. Chem. Phys. 48, 4946 (1968).

[b] D.L. Albritton, A.L. Schmeltekopf, and R.N. Zare, Diatomic Intensity Factors, in preparation.

Table IV. Coefficients of the important configurations in the approximate first-order wave functions for the lowest $^3\Pi_u$ and B $^3\Sigma_u^-$ states of $O_2$. The "degeneracy" is the number of $^3\Pi_u$ or $^3\Sigma_u^-$ symmetry eigenfunctions which arise from a given orbital occupancy, and the effects of all such eigenfunctions are included in the tabulated coefficients.

| | Orbital Occupancy | Degeneracy | Coefficient as a Function of Internuclear Separation (bohrs) | | |
|---|---|---|---|---|---|
| | | | 2.5 | 3.1 | 3.5 |
| | $^3\Pi_u$ | | | | |
| 1. | $2\sigma_g^2\ 2\sigma_u^2\ 3\sigma_g^2\ 3\sigma_u 1\pi_u^4\ 1\pi_g$ | 1 | 0.9328 | 0.8625 | 0.7653 |
| 2. | $2\sigma_g^2\ 2\sigma_u^2\ 3\sigma_g^2\ 3\sigma_u 1\pi_u^2\ 1\pi_g^3$ | 4 | 0.2963 | 0.4244 | 0.5204 |
| 3. | $2\sigma_g^2\ 2\sigma_u^2\ 3\sigma_g 3\sigma_u^2\ 1\pi_u^3\ 1\pi_g^2$ | 4 | 0.1191 | 0.1923 | 0.2897 |
| 4. | $2\sigma_g^2\ 2\sigma_u^2\ 3\sigma_g 3\sigma_u^2\ 1\pi_u 1\pi_g^4$ | 1 | 0.0498 | 0.1359 | 0.2112 |
| 5. | $2\sigma_g^2\ 2\sigma_u^2\ 3\sigma_g^2\ 3\sigma_u 1\pi_u^3\ 1\pi_g 2\pi_u$ | 9 | 0.0706 | 0.0608 | 0.0511 |
| 6. | $2\sigma_g^2\ 2\sigma_u^2\ 3\sigma_g^2\ 3\sigma_u 1\pi_u 1\pi_g^3\ 2\pi_u$ | 9 | 0.0432 | 0.0516 | 0.0463 |
| 7. | $2\sigma_g^2\ 2\sigma_u^2\ 3\sigma_g 3\sigma_u 4\sigma_g 1\pi_u^4\ 1\pi_g$ | 3 | 0.0387 | 0.0457 | 0.0409 |

Table IV Cont'd.

| B $^3\Sigma_u^-$ | | 2.5 | 3.1 | 3.5 |
|---|---|---|---|---|
| 1. $2\sigma_g^2\ 2\sigma_u^2\ 3\sigma_g^2\ 1\pi_u^3\ 1\pi_g^3$ | 1 | 0.8943 | 0.8121 | 0.7531 |
| 2. $2\sigma_g^2\ 2\sigma_u^2\ 3\sigma_g 3\sigma_u 1\pi_u^4\ 1\pi_g^2$ | 2 | 0.3671 | 0.4898 | 0.5256 |
| 3. $2\sigma_g^2\ 2\sigma_u^2\ 3\sigma_g 3\sigma_u 1\pi_u^2\ 1\pi_g^4$ | 2 | 0.1563 | 0.2403 | 0.3006 |
| 4. $2\sigma_g^2\ 2\sigma_u^2\ 3\sigma_g^2\ 3\sigma_u^2\ 1\pi_u^3\ 1\pi_g$ | 1 | 0.0464 | 0.0903 | 0.1425 |
| 5. $2\sigma_g^2\ 2\sigma_u^2\ 3\sigma_g^2\ 1\pi_u^2\ 1\pi_g^3\ 2\pi_u$ | 4 | 0.1048 | 0.0889 | 0.0716 |
| 6. $2\sigma_g^2\ 2\sigma_u^2\ 3\sigma_g^2\ 1\pi_u^4\ 1\pi_g 2\pi_u$ | 1 | 0.0979 | 0.0623 | 0.0463 |
| 7. $2\sigma_g^2\ 2\sigma_u^2\ 3\sigma_g^2\ 3\sigma_u^2\ 1\pi_u 1\pi_g^3$ | 1 | 0.0258 | 0.0551 | 0.0995 |
| 8. $2\sigma_g^2\ 2\sigma_u^2\ 3\sigma_u^2\ 1\pi_u^3\ 1\pi_g^3$ | 1 | 0.0187 | 0.0454 | 0.1180 |

Table V. Natural orbital occupation numbers for the $^3\Pi_u$ and B $^3\Sigma_u^-$ states for $O_2$ as a function of internuclear separation, in bohrs.

| | | $2\sigma_g$ | $2\sigma_u$ | $3\sigma_g$ | $3\sigma_u$ | $4\sigma_g$ | $4\sigma_u$ | $1\pi_u$ | $1\pi_g$ | $2\pi_u$ | $2\pi_g$ |
|---|---|---|---|---|---|---|---|---|---|---|---|
| $^3\Pi_u$ | r=2.5 | 1.998 | 1.993 | 1.973 | 1.015 | 0.004 | 0.002 | 3.779 | 1.224 | 0.009 | 0.002 |
| | r=3.1 | 1.998 | 1.997 | 1.935 | 1.057 | 0.005 | 0.001 | 3.521 | 1.474 | 0.009 | 0.002 |
| | r=3.5 | 1.999 | 1.999 | 1.864 | 1.130 | 0.004 | 0.001 | 3.219 | 1.775 | 0.006 | 0.002 |
| B $^3\Sigma_u^-$ | r=2.5 | 1.997 | 1.994 | 1.829 | 0.184 | 0.001 | 0.001 | 3.109 | 2.856 | 0.024 | 0.005 |
| | r=3.1 | 1.996 | 1.992 | 1.685 | 0.347 | 0.002 | 0.001 | 3.175 | 2.783 | 0.015 | 0.004 |
| | r=3.5 | 1.996 | 1.994 | 1.594 | 0.474 | 0.002 | 0.001 | 3.165 | 2.761 | 0.010 | 0.003 |

## Figure Captions

1. Theoretical potential curves for the $^3\Pi_u$, $^1\Pi_u$, and B $^3\Sigma_u^-$ states of $O_2$. The experimental B state curve is that of Albritton, et.al., reference 28. The dashed line is the repulsive curve inferred by Murrell and Taylor (reference 15). The energy scale is relative to the v=0 level of the X $^3\Sigma_g^-$ ground state.

2. A sketch of some repulsive curve $V_2(r)$ crossing (a) the outer branch and (b) the inner branch of the bound potential $V_1(r)$. The shaded regions are the "potential wells" associated with the phase integral $\tau$, defined by Eq. (12) for case (a) and Eq. (13) for case (b).

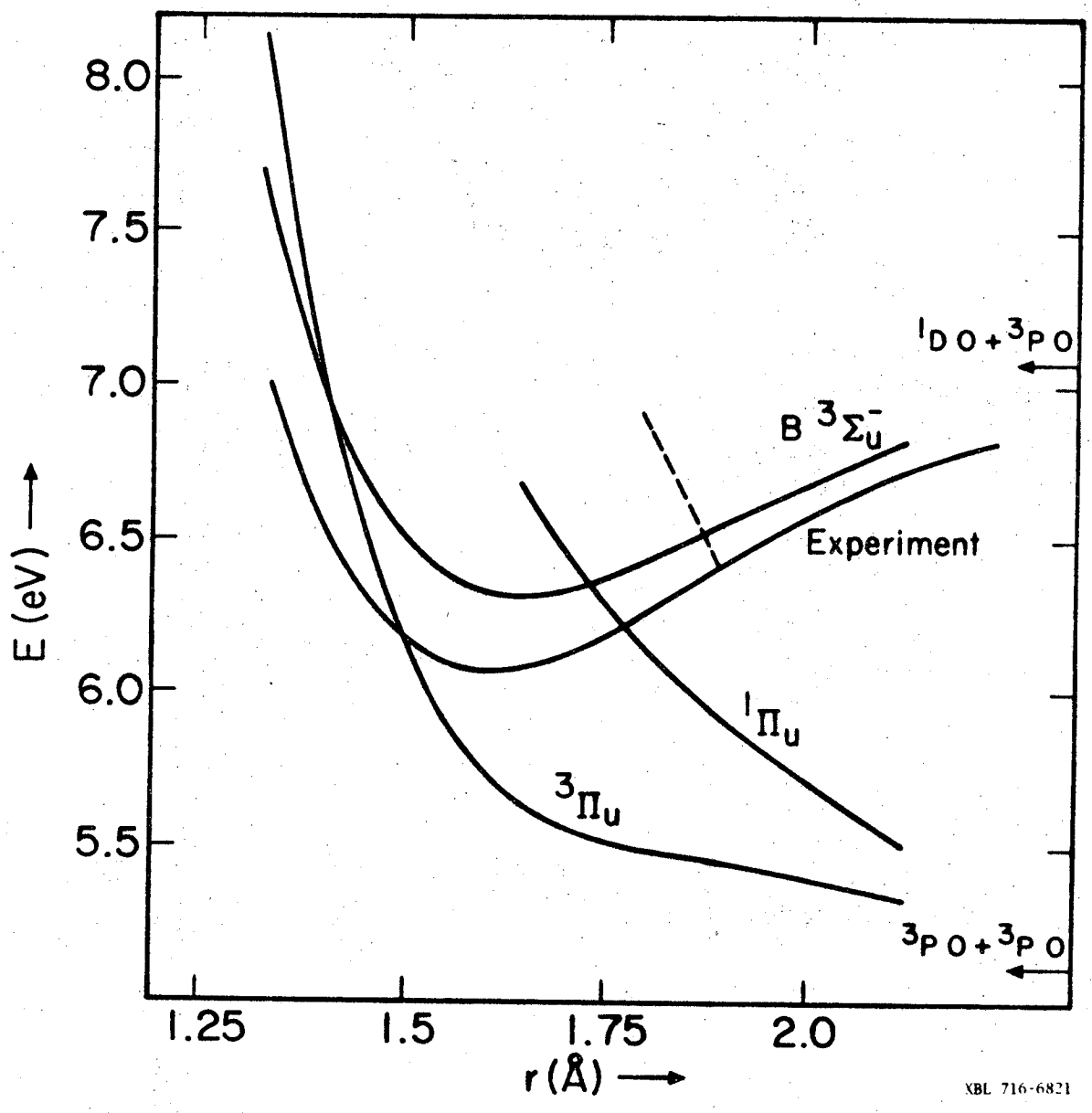
8.0
7.5
7.0
6.5
6.0
5.5
E (eV)
1.25
1.5
1.75
2.0
r (Å)
$^1D\,O + {}^3P\,O$
$B\,{}^3\Sigma_u^-$
Experiment
$^1\Pi_u$
$^3\Pi_u$
$^3P\,O + {}^3P\,O$
XBL 716-6821

Figure 1.

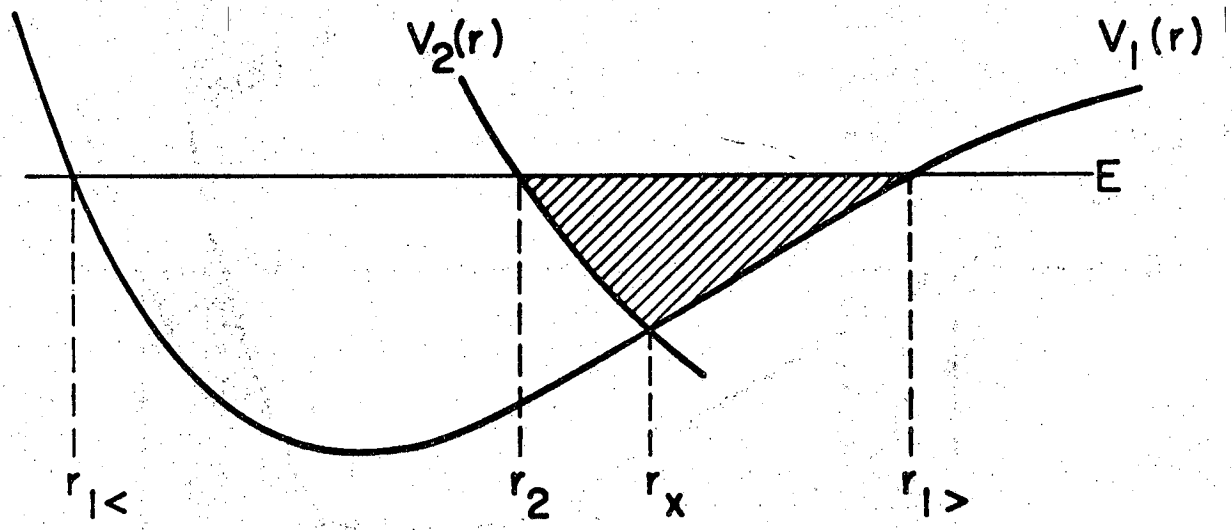


(a)

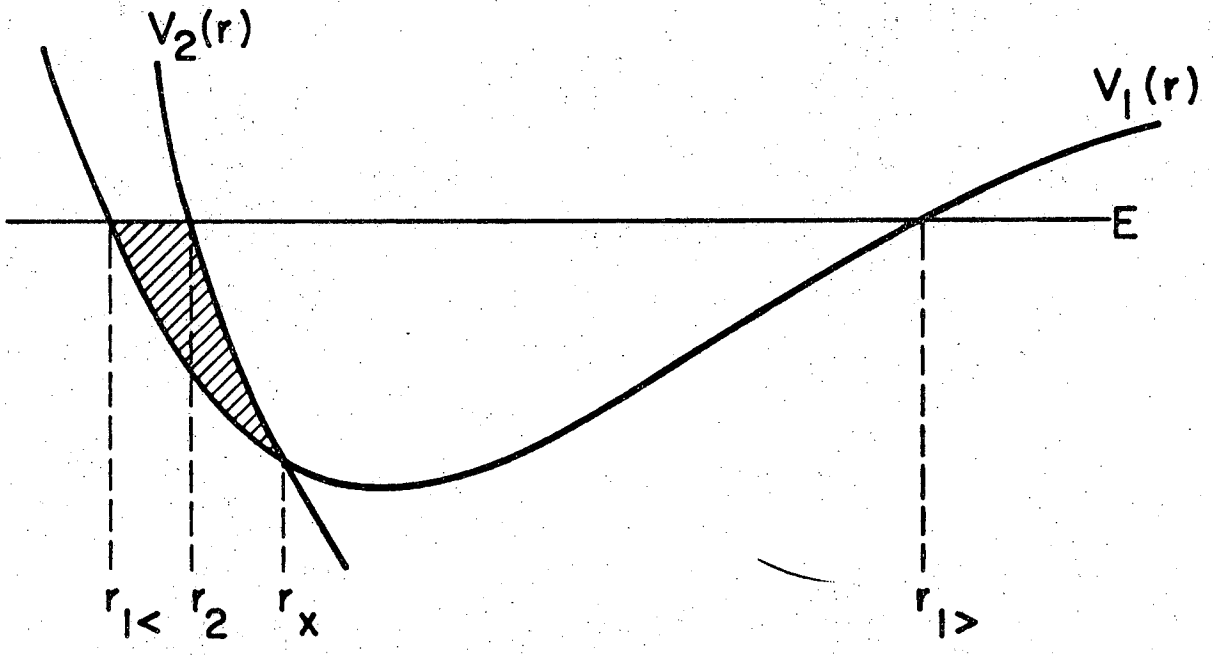


(b)

XBL 716-6822

Figure 2.

TECHNICAL INFORMATION DIVISION
LAWRENCE RADIATION LABORATORY
UNIVERSITY OF CALIFORNIA
BERKELEY, CALIFORNIA 94720